Virchows Arch [Pathol Anat] (1984) 405:25–39

Virchows Archiv A

A morphometric study on the ultrastructure of well-differentiated tumours and inflammatory mucosa of the human urinary bladder

Nobuo Moriyama[1], Masao Yokoyama[2], and Tadao Niijima[1]

[1] Department of Urology, Faculty of Medicine, The University of Tokyo, Hongo, Bunkyo-ku, Tokyo, 113,
[2] Department of Urology, Toranomon Hospital, Minato-ku, Tokyo, Japan

Summary. Transmission (TEM) and scanning electron microscopic (SEM) observations were performed on well-differentiated tumours and chronic cystitis in the human urinary bladder. SEM showed that the pleomorphic microvilli were present not only on the luminal surface of the tumour but also on the surface of inflammatory mucosa. The ultrastructure of six tumours and 5 cases of chronic cystitis was evaluated morphometrically. Bladder tumour and inflammatory mucosa were divided into several layers, namely outermost cells (S), subsurface cells just beneath these (S1), subsurface cells of 2 or 3 layers below (S23), intermediate cells of 2 or 3 layers above the basal cells (I23), intermediate cells just above the basal cells (I1) and basal cells (Ba). Areas of nucleus, cytoplasm and cytoplasmic organelles, numbers of nucleoli, nuclear bodies, mitochondria and lysosomes together with irregularity of the cell and nucleus were estimated according to the methods of Weibel. A multivariate analysis of variance on these variables showed that the above subdivision of layers was necessary for the comparison of tumour and inflammation. Discriminant analysis showed various differences between tumour and inflammatory mucosa. The results indicated that the Ba layer is the most effective site for differentiating the tumour from inflammation. Ba cells with large and irregular cytoplasm with an enlarged Golgi area, accompanied by many vacuolar structures, may be indicative of tumour rather than inflammation.

Key words: Morphometry – Human bladder tumour – Human chronic cystitis – Ultrastructure

Currently multiple random biopsy of the bladder mucosa is performed to order to find early lesions of transitional cell cancer since the tumours arise multicentrically (Soloway et al. 1978; Wolf and Hojgaard 1980). For

Offprint requests to: N. Moriyama at the above address

this purpose it is important to discriminate a well-differentiated bladder tumour from chronic inflammation with hyperplasia. However, non-tumorous lesions of the human bladder mucosa have rarely been studied by electron microscopy. An increase in the epithelial cell layers and a presence of pleomorphic microvilli by scanning electron microscopy (SEM) on the outermost cells have been proposed as the characteristic features of bladder tumours (Jacobs et al. 1976 and 1981). However, these features were also present in reversible hyperplasia of the rat urinary bladder (Fukushima et al. 1981). At present there seems to be no definite discriminating point between these two lesions. This study was performed to compare the ultrastructure of well-differentiated bladder tumours and chronic cystitis accompanied by hyperplasia. Further, morphometric studies using a multipurpose grid (Weibel 1969) were performed on the cytoplasmic area, nuclear area, and numbers and area of cytoplasmic organellae. A discriminant analysis (Solberg et al. 1982) was employed for the differential recognition of tumour and inflammatory lesions.

Materials and methods

Six cases of well-differentiated bladder tumour (G1:5, G2:1) and 5 cases of chronic cystitis with hyperplasia surved for the study. These 5 cases had no history of bladder tumours before the biopsies, and showed no development of tumours during a mean follow up of 1 year (range 0.5–1.5). The specimen was obtained by cold punch biopsies under spinal or epidural anesthesia. For light microscopic observation specimens were fixed with 10% formalin and paraffin embedded tissues were stained with haematoxylin and eosin. For transmission electron microscopic (TEM) examination, specimens were fixed in a modified Karnovsky's fixative (1% paraformaldehyde and 2.5% glutaraldehyde solution) and postfixed in 2% osmium tetroxide solution. They were dehydrated in an ascending series of alcohol and embedded in Epon 812. Ultrathin sections were cut and stained doubly with uranyl acetate and lead citrate. Observations were performed in a Hitachi 100B electron microscope with a direct magnification of 2,400–4,800 ×. Morphometry was done on the pictures enlarged up to 7,200 ×. For scanning electron microscopic (SEM) observation, specimens were similarly fixed and dehydrated. They were transferred into isobutyl acetate and dried in a critical point drying apparatus using liquid cabon dioxide. After mounting on aluminum stubs, specimens were coated with gold, and examined with a Hitachi S 430 scanning electron microscope at 15–25 KV.

Morphometrical method

Cell layers of both tumour tissues and inflammatory mucosa of human bladder were subdivided into the following 6 groups. The outermost cells (S) were designated as the cells facing the bladder lumen. Subsurface cells (S1) and lower cells (S23) were identified as 1 and 2–3 layers beneath the outermost cells, respectively. Basal cells (Ba) were the ones which were located just above the basement membrane. Intermediate cells (I1, I23) were defined as the cells 1 and 2–3 layers above the basal cells, respectively. These subdivisions of cell layers were carried out on each micrograph. About forty cells in each patient (about 7 cells per each layer) were randomly selected. Areas of each cell, nucleus, cytoplasmic vacuolar structure, Golgi apparatus and rough endoplasmic reticulum (rough-ER) were measured using 5 mm intervals of the multipurpose grid superimposed on the micrographs enlarged to 7,200 ×. The point counting method was employed (Weibel 1969). Numbers of mitochondria, lysosomes, nucleus and nuclear bodies per cell were also counted. Nuclear and cellular irregularity were estimated with the following irregularity index (Higashi 1969).

Irregularity index = R/r, where $R = x/2\pi$, $r = \sqrt{y/\pi}$ and x and y denote nuclear circumference and nuclear area, respectively.

The nuclear cytoplasmic ratio (N/C) was calculated with a division of nuclear area by cytoplasmic area. Each calculated variable was tested with the Student's *t*-test.

A multivariate analysis on tumour and inflammatory mucosa of human bladder

For this analysis, the variables calculated above were used. N/C ratio was excluded because it was not the independent factor. A multivariate analysis of variance (MANOVA) (Potthoff and Roy 1964) was applied to test whether the observed differences among the means of the 6 layers (S, S1, S23, I23, I1, Ba) were by chance or these differences were indicative of actual differences of means among the corresponding population. The numbers of cells in each layer were 41 in tumour case and 38 in inflammation cases, respectively. The data sets were treated as variables. MANOVA of one way allocation was used to test the hypothesis that the population means of 6 layers were all equal. A multiple comparison method was applied to compare the means of the each layer. Discrimination between tumour and inflammatory epithelium of human bladder was attempted using the discriminant analysis (stepwise forward method) (Solberg et al. 1982). Discriminant analysis is a method to divide all the samples into some groups. Discriminant functions were set in order to minimize the probability of misclassification (rate of misdiagnosis when the given variables were used for differentiation).

Results

1. Ultrastructure

1. Tumours. Well-differentiated tumours were composed of about 10 layers of cells. The outermost cells were cuboidal in shape. Intermediate and basal cells were spindle-shaped with the long axis perpendicular to the basement membrane. The luminal surface of the outermost cells possessed numerous microvilli. Discoid vesicles were not seen. Mitochondria were located at the supranuclear position. Rough-ER were not conspicuous. Secondary lysosomes were scattered in the cytoplasm. Shapes of nuclei were ovoid and slightly irregular. One or several small nucleoli were found in a nucleus. Heterochromatin granules were not conspicuous. The findings of the intermediate and basal cells appeared similar to those of the outermost cells. Basal cells were enlarged in size (Figs. 1 and 2).

SEM observation revealed that the luminal surface of the outermost cells were similar in size and polygonal in shape. Luminal surfaces were covered by pleomorphic microvilli of various shapes and sizes (Fig. 5).

2. Chronic cystitis. Inflammatory epithelia were composed of 6–8 layers of cells. Outermost cells appeared cuboidal, while the intermediate and basal cells were spindle-shaped and similar to the corresponding tumour layers. An inflammatory infiltrate predominantly composed of lymphocytes and polymorphonuclear leucocytes with oedema were recognized in the submucosal area.

TEM observation showed the outermost cells to have many microvilli on their surface. The discoid vesicles were not observed (Fig. 3). Rough-ER was abundant in the supranuclear areas. Mitochondria were scattered in the supranuclear area. Nuclei were deeply notched and irregular in shape. Nucleoli were conspicuous in some cells. Heterochromatin granules were

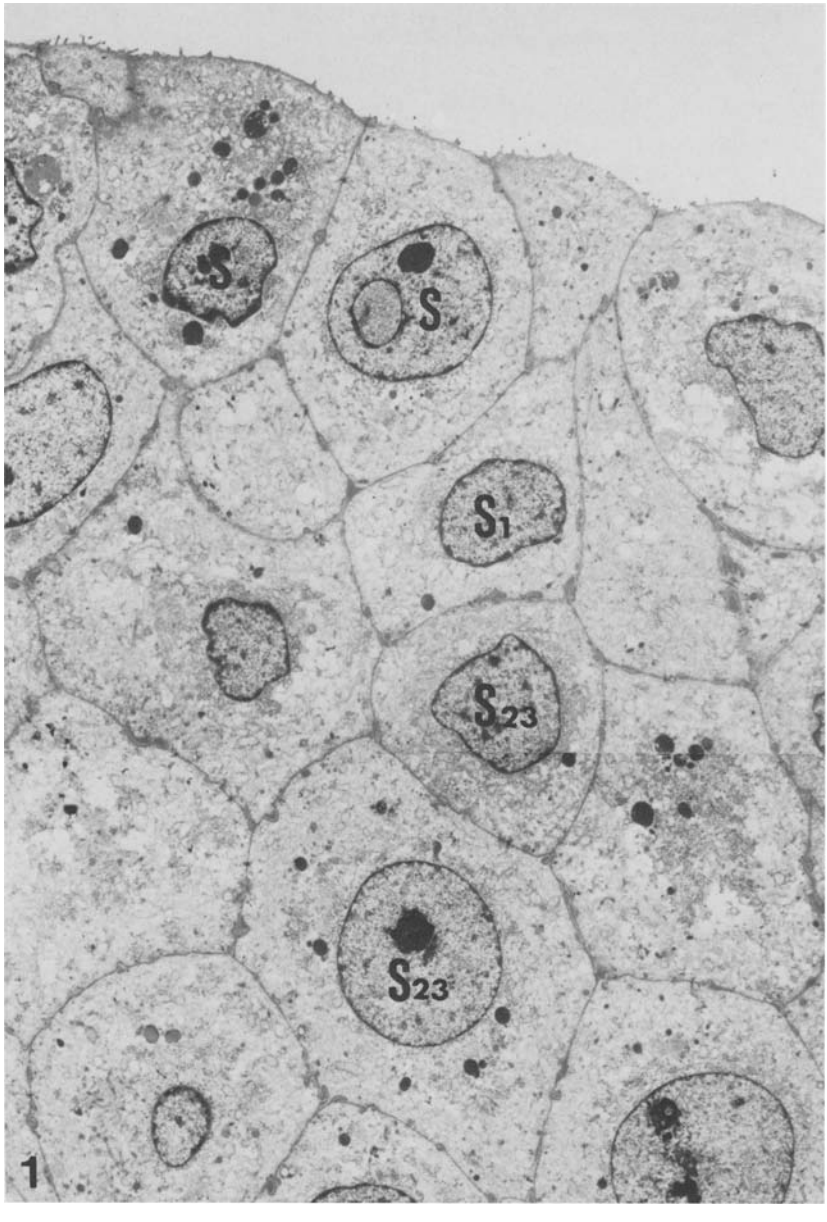

Fig. 1. Upper cell layers of a tumour in human urinary bladder revealed by TEM. Cytoplasm and nuclei of upper cell layers of bladder tumour were large. ×3,600. *S*, outermost cells; *S1*, cells of just beneath the outermost cells; *S23*, cells of 2 or 3 layers underneath

not outstanding. Intermediate and basal cells appeared similar as was the case in the tumour tissues (Figs. 3 and 4), although the cytoplasm of these cells was slightly smaller.

SEM observation revealed that the outermost cells were uniform in size and polygonal in shape. Microvilli diffusely covered the cell surface. They

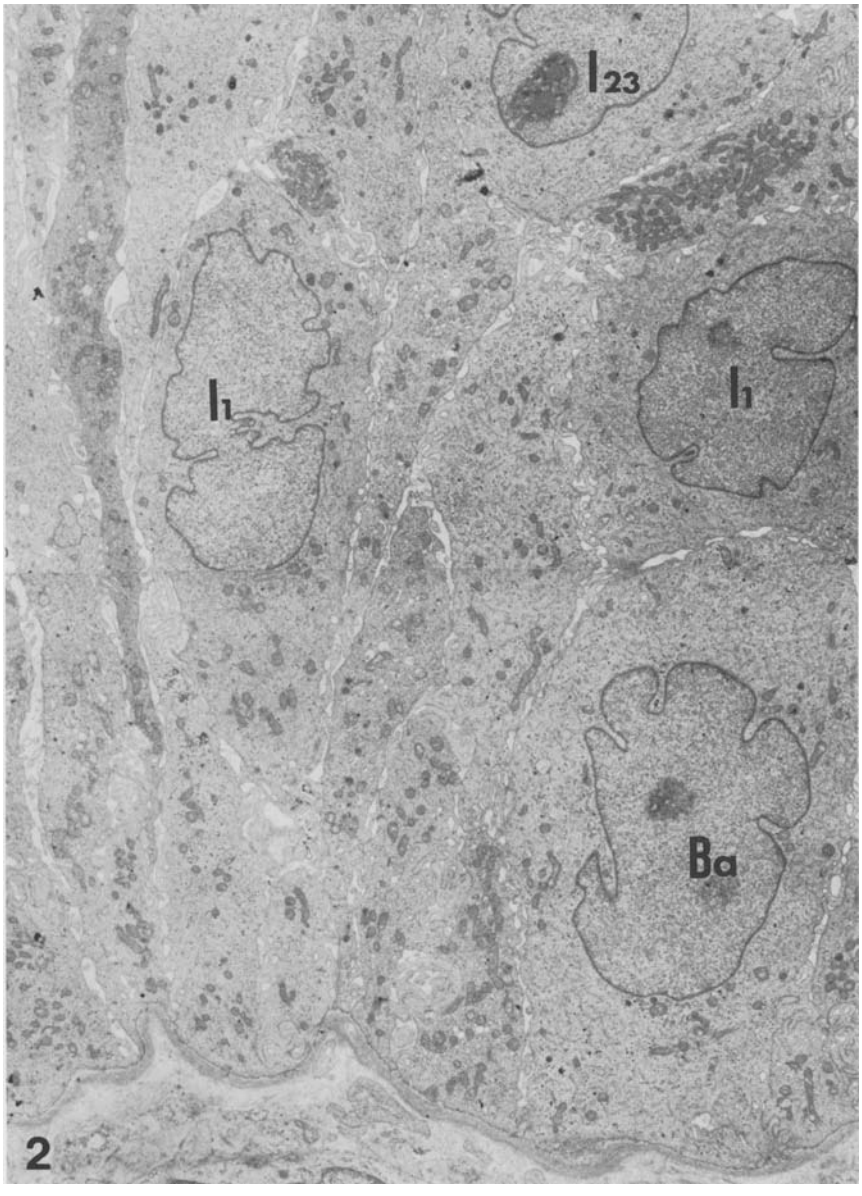

Fig. 2. Lower cell layers of a tumour in human urinary bladder revealed by TEM. Basal cells were enlarged. ×3,600. *I23*, cells of 2 or 3 layers above the basal cells; *I1*, cells of just above them; *Ba*, basal cells

were straight and uniform in appearance although their hight were variable. Pleomorphic microvilli were found in two cases (Fig. 6).

2. Morphometry

Means and standard deviations of the nuclear cytoplasmic (N/C) ratio, nuclear areas, cytoplasmic areas, numbers of lysosomes per cell, Golgi areas

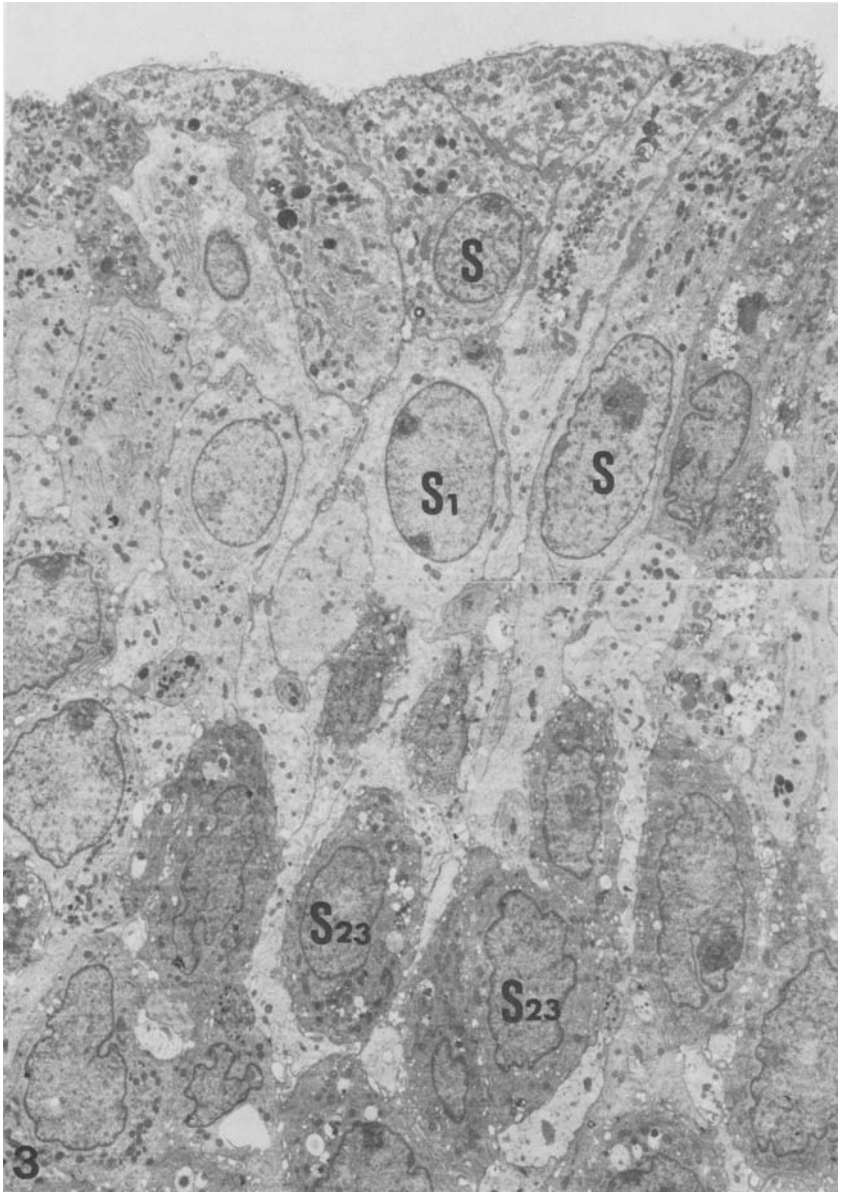

Fig. 3. Upper cell layers of inflammatory epithelium of human urinary bladder revealed by TEM. Outermost cells were cuboidal and have microvilli. ×3,600. Abbreviations are same as in Fig. 1

and rough-ER areas in tumourous and inflammatory mucosa were summarized in Tables 1–6. The N/C ratios of I23, I1 and Ba layers of the tumour were significantly smaller than that of the inflammation ($P<0.05$, $P<0.01$ and $P<0.01$, respectively) (Table 1). The nuclear areas of the tumour were significantly larger than those of the inflammation in S23, I23 and Ba layers

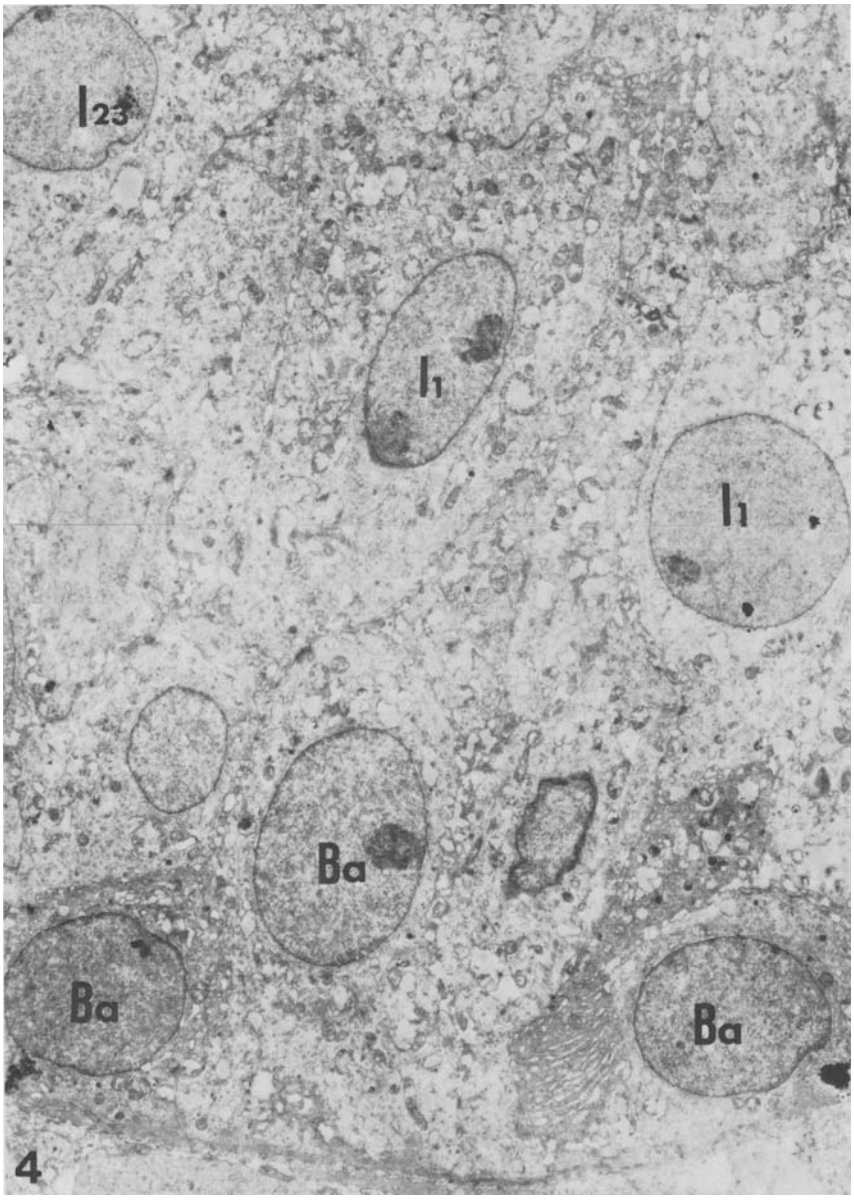

Fig. 4. Lower cell layers of inflammatory epithelium of human urinary bladder revealed by TEM. Intermediate and basal cells were relatively small. ×3,600. Abbreviations are same as in Fig. 2

($P<0.05$) (Table 2). The cytoplasmic areas of I23, I1 and Ba layer of tumours were significantly larger than those of inflammation ($P<0.01$) (Table 3). The Numbers of lysosomes in the I1 layer of the tumour were significantly higher than those of inflammation ($P<0.05$) (Table 4). The Golgi areas were significantly larger in tumour cells than in inflammatory cells

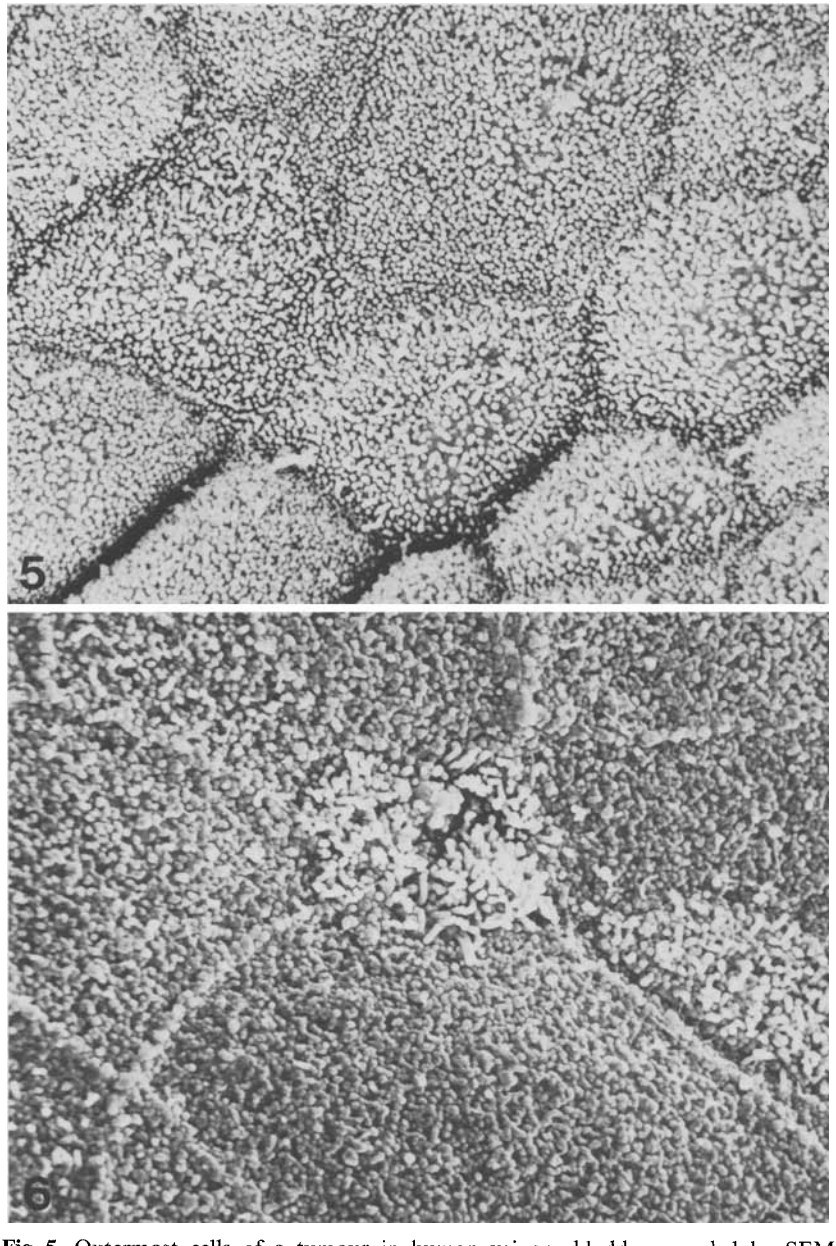

Fig. 5. Outermost cells of a tumour in human urinary bladder revealed by SEM. Diffuse microvilli of various sizes and shapes were observed. Some showed pleomorphism. × 4,200

Fig. 6. Outermost cells of inflammatory epithelium of human urinary bladder revealed by SEM. Short stabby microvilli were observed on the outermost cells. Pleomorphic microvilli were also observed. × 4,200

Table 1. Nuclear cytoplasmic ratio ($\mu m^2/\mu m^2$)

	Tumour (6 cases) $n=41$	Inflammation (5 cases) $n=38$
S	0.334±0.162	0.328±0.179
S1	0.380±0.206	0.405±0.240
S23	0.432±0.211	0.456±0.418
I23*	0.501±0.342	0.710±0.482
I1**	0.450±0.308	0.762±0.445
Ba**	0.363±0.235	0.515±0.248

*$P<0.05$ **$P<0.01$

Table 2. Nuclear area (μm^2)

	Tumour (6 cases) $n=41$	Inflammation (5 cases) $n=38$
S	36.13±17.63	31.96±13.57
S1	31.93±13.25	29.26±15.40
S23*	35.10±15.15	28.18±13.56
I23*	30.82±15.20	25.37±12.94
I1	29.17±12.49	30.46±13.99
Ba*	34.07±16.02	27.46±14.66

*$P<0.05$, **$P<0.01$

Table 3. Cytoplasmic area (μm^2)

	Tumour (6 cases) $n=41$	Inflammation (5 cases) $n=38$
S	121.53±56.58	113.68±53.45
S1	98.96±50.34	91.63±64.61
S23	94.79±46.60	80.79±44.82
I23**	82.22±47.74	46.65±29.82
I1**	89.74±53.54	57.17±45.10
Ba**	116.65±59.81	57.95±29.23

*$P<0.05$, **$P<0.01$

Table 4. Number of lysosome (/cell)

	Tumour (6 cases) $n=41$	Inflammation (5 cases) $n=38$
S	2.0±2.9	1.9±2.9
S1	1.0±2.1	1.2±2.5
S23	0.9±2.1	1.2±2.3
I23	1.2±3.0	0.4±1.8
I1*	0.8±1.7	0.2±0.6
Ba	0.3±0.9	0.6±2.9

*$P<0.05$, **$P<0.01$

Table 5. Golgi area (μm^2)

	Tumour (6 cases) $n=41$	Inflammation (5 cases) $n=38$
S*	0.754 ± 1.376	0.253 ± 0.611
S1	0.397 ± 1.253	0.099 ± 0.610
S23**	0.968 ± 2.051	0.055 ± 0.198
I23**	0.733 ± 1.245	0.055 ± 0.339
I1	0.570 ± 1.169	0.187 ± 0.691
Ba*	0.713 ± 1.233	0.209 ± 0.725

*$P<0.05$, **$P<0.01$

Table 6. Rough-ER area (μm^2)

	Tumour (6 cases) $n=41$	Inflammation (5 cases) $n=38$
S	4.869 ± 7.285	8.231 ± 11.246
S1	3.616 ± 4.329	3.703 ± 6.185
S23	3.382 ± 5.693	2.583 ± 3.515
I23	2.750 ± 3.312	1.703 ± 2.831
I1	2.434 ± 3.040	2.528 ± 4.981
Ba**	3.310 ± 3.423	1.132 ± 1.875

*$P<0.05$, **$P<0.01$

in S, S23, I23 and Ba layers ($P<0.05$, $P<0.01$, $P<0.01$ and $P<0.05$, respectively) (Table 5). In Ba layers, the area of rough-ER of the tumour was significantly larger than that of the inflammation cases ($P<0.01$) (Table 6).

3. A multivariate analysis

1. MANOVA (Multivariate analysis of variance). Hypothesis of the equality of all layers was rejected both in tumour and inflammation by MANOVA (Tumour: $P<0.01$; Inflammation: $P<0.01$). In the multiple comparison method, all combinations between upper layers (S, S1 and S23) and lower layers (I23, I1 and Ba) showed a significant differences both in tumour and in inflammation (Tumour: $P<0.01$; Inflammation: $P<0.01$). Outermost cells (S) differed significantly from S1 layer in tumour as well as in inflammation (Tumour: $P<0.05$; Inflammation $P<0.01$). The significant difference between the I1 layer and basal layer as well as between the I23 layer and basal layer were recognized in the tumours ($P<0.01$). The outermost cells (S) were significantly different from S1 and S23 layers respectively, in inflammation ($P<0.01$) (Table 7).

2. Discriminant analysis. Table 8 showed the result of discriminant analyses with the probability of misclassification and partial correlation coefficients (Plus shows the direction of the tumour). The meaning of absolute values

Table 7. Multivariate analysis of variance and multiple comparison among layers of tumour and inflammation

Hypotheses	Tumour (statistics X_0^2)	Inflammation (statistics X_0^2)
MANOVA		
H0: All layers are same	121.6**	204.53**
Multiple comparison		
H1: S = S1	23.6*	67.4**
H2: S, S1 = S23	14.5	49.00**
H3: S, S1, S23 = I23, I1, Ba	43.1**	96.2**
H4: I23 = I1	14.6	15.4
H5: I23, I1 = Ba	27.3**	6.3

* Hypotheses are rejected with $P<0.05$
** Hypotheses are rejected with $P<0.01$

Table 8. Partial correlation coefficients of discriminant analysis between tumour and inflammation

Mis-classfi. rate (%)		Partial correlation coefficients										
		A	B	C	D	E	F	G	H	I	J	K
S	30	0.335				−0.368		−0.317	−0.266	−0.332		
S1	34								0.242		0.261	−0.293
S23	42	0.194					0.266					
I23	27		0.341			−0.196	0.259	−0.180	0.181	−0.300	0.266	
I1	29		0.408		0.328			−0.341	−0.170	0.199		0.165
Ba	25	−0.230	0.508		0.230		0.300					0.420

Plus shows the direction for tumour.

A: nuclear areas, B: cytoplasmic areas, C: numbers of lysosome, D: areas of vacuolar structure, E: numbers of mitochondria, F: Golgi areas, G: areas of rough-ER, H: numbers of nucleolus, I: numbers of nuclear body, J: nuclear irregularity, K: cellular irregularity

is as follows: if the values are large in some variables, these contribute heavily for differentiation).

According to the probability of misclassification, the Ba layer showed the best differentiation (25% of misclassification rate) and I23 layer is the second (27%). Important variables of the Ba layer for discrimination were area of cytoplasm, irregularity of cells, area of Golgi, area of nuclei and vacuolar structures (partial correlation coefficient 0.508, 0.420, 0.300, −0.230 and 0.230, respectively) (Table 8). Tumour cells of the basal layer were recognized as large and irregular cells containing enlarged Golgi areas and numerous vacuolar structures, while inflammatory Ba cells have relatively large nuclei. Generally, tumour cells have large cytoplasm (I23, I1 and Ba) with enlarged Golgi area (S23, I23 and Ba). Inflammatory cells, on the other hand, have enlarged area of rough-ER. (S, I23 and I1) and increased number of mitochondria (S and I23).

Discussion

It is important to differentiate between early lesions of the transitional cell carcinoma and the chronic inflammation in bladder biopsies, though it is contraversial whether chronic inflammation is a precancerous lesion in transitional cell carcinoma, especially in humans who have no past history or presence of tumour. Inflammatory lesions sometimes simulate the tumour and accompany the hyperplasia which also relates to it and is the source of papillary neoplasia (Koss 1975). However it is not so easy to distinguish the well-differentiated papillary carcinoma from chronic cystitis with simple hyperplasia at the morphological level. The inflammation of the bladder usually has an infiltration of inflammatory cells and oedema in the submucosal area. The bladder tumour frequently is accompanied by the same finding, this may be of no help for the differential diagnosis between the tumour and inflammation. Pleomorphic microvilli have been known to be prominent in the outermost cells of bladder tumours (Jacobs et al. 1976 and 1981). Pleomorphic microvilli are longer and broader than regular microvilli (Nelson et al. 1979) and are branched with bulbous tips (Jacobs 1982). However, pleomorphic microvilli have also been reported in reversible hyperplasia (Fukushima et al. 1981). They were also found in non-tumour lesion of the human urinary bladder (Anderstrom et al. 1984). The present study showed the presence of pleomorphic microvilli on the luminal surface of the chronic cystitis (Fig. 6). These findings indicate that pleomorphic microvilli are not an absolute marker in human and experimental bladder tumours.

TEM and SEM observations of the benign lesions of the human urinary bladder have rarely been reported. Collan et al. (1976) reported electron microscopic observations in interstitial cystitis but did not mention the nature of the outermost cells. SEM study by Kjaergaard et al. (1977) showed the outermost cells of cystitis to be smooth without microstructures. Haynes (1975) observed a decrease of lysosomes and increase of rough-ER in the inflammatory bladder mucosa in children, but she did not describe the surface structure. Skolda et al. (1974) also reported smooth outermost cells on experimental cystitis induced by E. coli. These smooth cells were considered to be necrotic epithelium. The present study deals with chronic cystitis with cellular proliferation which may represent a kind of simple hyperplasia. Therefore, the cellular behavior may be different from exfoliative acute cystitis.

Nuclear irregularities and N/C ratios have also been considered to be indications of malignancy, especially in the field of cytology (Papanicolou 1963). The cytology of well-differentiated bladder tumours, however, usually results in the diagnosis of class 1 or 2 changes. The differential diagnosis of these two diseases is not easy in cytology or histology. These facts were supported by the present analysis of the N/C ratio, since the Student's *t*-test failed to show a difference between these ratios for tumour and inflammation in surface layers (S, S1 and S23) (Table 1).

Morphometric studies have been done on human bladder tumours (Fulker et al. 1976; Ooms et al. 1981; Smith 1981 and 1982). Fulker et al. (1976) reported that some tumours showed higher values for nuclear profile areas and less invaginated nuclear configuration than normal bladder epithelium. Ooams et al. (1981) reported the prognostic significance of morphometry in T1 bladder tumours. Smith (1981) observed the higher percentages of reduplication of the basal lamina and of discontinuous basal lamina in tumours than in normal bladder epithelium. In his succeeding report, he showed an increase in the immature, small dark cells in the superficial layers of the tumour (Smith 1982). Morphologically, normal bladder epithelium has been divided into surface cells, intermediate cells and basal cells depending on their location (Fulker et al. 1971). The bladder mucosa in pathological conditions has also been divided in the same manner. The importance of these subdivisions of cell layers in tumour and inflammatory mucosa of human urinary bladder was clearly shown in the present study using MANOVA.

Multivariate analysis is a method to analyse the total correlations of many variables. It may show the difference when an individual variable has failed to reveal one in Student's *t*-test. This discriminant analysis has been utilized for the differential diagnosis of some diseases (Fraser et al. 1971; Solberg et al. 1975). The method is generally effective when a linear correlation is recognized between variables and groups. In the present study, this method was considered to be effective, although a linear correlation for each variable has not yet been verified. The analysis in the present study showed that the Ba layer was the most effective site at which to differentiate tumours from inflammation (25% of misclassification rate). Tumour cells have large cytoplasm with irregular shapes, enlarged Golgi areas and many vacuolar structures. Our previous study on the estimation of the cell areas of bladder epithelium showed similar results by the Student's *t*-test (Moriyama et al. 1980). Cellular irregularity may be due to an increase of intercellular cytoplasmic processes or microplicae, and can also be affected by the osmolarity of the fixative. The shrinkage of a large elongated basal cell may induce an increase in the cytoplasmic irregularity index. Our study showed an enlarged Golgi area in Ba layer of the tumour and was considered to be a good indication of a tumour cell. The Golgi complexs are known to synthesize fusiform vesicles in normal bladder epithelium, and may also therefore, have an important role in tumours. Although vacuolar structures are increased in the tumour cells of the Ba layers, the reliability of this variable is limited since the vacuoles could be a rough-ER and Golgi vesicles. Degenerated mitochondria could also be a potential origin for vacuolar structures. Lysosomes were reported to be abundant in normal superficial cells (Suzuki 1982), while they were reported as decreased in acute inflammation (Haynes et al. 1975). In the present study this variable was not useful in the differential diagnoses of bladder tumours and inflammation. It could be due to the fact that our materials showed chronic rather than acute inflammations. The present study showed an increase of rough-

ER area in inflammatory cells (S, I23 and I1). Kashiwai (1961) has already described similar findings, although morphometry was not performed.

Acknowledgement. The authors are indebted to Mr. Yuzo Fujitani of Kaken Chemical Co. for his help in statistical analysis. A part of this work was supported by a grant from the Japanese Ministry of education (57570573) to M. Yokoyama.

References

Anderstrom C, Ekelund P, Hansson HA, Johansson L (1984) Scanning electron microscopy of polypoid cystitis. A reversible lesion of the human bladder. J Urol 131:242–244

Collan Y, Alfthan O, Kivilaakso E, Oravisto KJ (1976) Electron microscopic and histological findings on urinary bladder epithelium in interstitial cystitis. Eur Urol 2:242–247

Fraser P, Healy M, Rose N, Watson L (1971) Discriminant analysis functions in differential diagnosis of hypercalcemia. Lancet I. 1314

Fukushima S, Cohen SM, Arai M, Jacobs JB, Friedell GH (1981) Scanning electron microscopic examination of reversible hyperplasia of the rat urinary bladder. Am J Pathol 102:373–380

Fulker MJ, Cooper EH, Tanaka T (1971) Proliferation and ultrastructure of papillary transitional cell carcinoma of the human bladder. Cancer 27:71–81

Fulker MJ, Adamthwaite SJ, Anderson CK (1976) Stereological measurements of bladder tumour morphology. Eur J Cancer 12:575–579

Haynes M, Trott PA, Islam AKMS, Hirst G (1975) An ultrastructural study of the urinary bladder in children correlated with histological, bacteriological, and clinical findings. J Clin Pathol 28:176–188

Higashi Y (1969) Electron microscopy of human thyroid tumor. J Clin Electron Microscopy 2:326–364

Jacobs JB (1982) AUM monographs vol 1-Bladder cancer: The potential of scanning electron microscopic (SEM) exfoliative cytology in the clinical management of human bladder cancer. 95–109

Jacobs JB, Arai M, Cohen SM, Friedell GH (1976) Early lesion in experimental bladder cancer: Scanning electron microscopy of cell surface markers. Cancer Res 36:2512–2517

Jacobs JB, Cohen SM, Farrow GM, Friedell GH (1981) Scanning electron microscopic features of human urinary bladder cancer. Cancer 48:1399–1409

Kashiwai K (1961) An electron microscopic study on the transitional cell carcinoma of human urinary bladder. Jpn J Urol 52:909–925 (Jap)

Kjaergaard J, Starklint H, Bierring F, Thybo E (1977) Surface topography of the healthy and diseased transitional cell epithelium of the human urinary bladder. Urol Int 32:34–48

Koss LG (1975) Tumor of the urinary bladder. Atlas of tumor pathology, fascicle 11, 2nd series. Armed Forces Institute of Pathology. Washington, DC

Moriyama N, Yokoyama M, Niijima T (1980) Electron microscopic morphometry on the nucleus of human bladder tumor and infection. J Clin Electron Microscopy 13:781–782

Nelson CE, Croft WA, Nilsson T (1979) Surface characteristics of malignant human urinary bladder epithelium studied with scanning electron microscopy. Scand J Urol Nephrol 13:31–42

Ooms ECM, Essed E, Veldhuizen RW, Alons CL, Kurver P, Boon ME (1981) The prognostic significance of morphometry in T1 bladder tumours. Histopathology 5:311–318

Papanicolau GN (1963) Atlas of exfoliative cytology. Harvard Univ Press, Cambridge

Potthoff RF, Roy SN (1964) A generalized multivariate analysis of variance model useful especially for growth curve problems. Biometrika 51:313–326

Skoluda D, Richter IE, Busse K (1974) Experiments in Coli cystitis. Urol Int 29:299–311

Smith AF (1981) An ultrastructural and morphometric study of bladder tumors (I). Virchows Arch [Pathol Anat] 390:11–21

Smith AF (1982) An ultrastructural and morphometric study of bladder tumours (II). Virchows Arch [Pathol Anat] 396:291–301

Solberg HE, Skrede S, Blomhoff JP (1975) Diagnosis of liver diseases by laboratory results and discriminant analysis. Scand J Clin Lab Invest 35:713–721

Solberg HE, Skrede S, Rootwelt K (1982) The use of discriminant and other multivariate statistical methods for the identification of efficient combinations of laboratory tests. Clin Lab Med 2:735–750

Soloway MS, Murphy W, Rao MK, Cox C (1978) Serial multiple-site biopsies in patients with bladder cancer. J Urol 120:57–59

Suzuki T (1982) A scanning and transmission electron microscopic study on the human normal urinary bladder and bladder tumors. Jpn J Urol 73:469–487 (Jap)

Weibel ER (1969) Stereological principles for morphometry in electron microscopic cytology. Int Rev Cytol 26:235–302

Wolf H, Hojgaad K (1980) Urothelial dysplasia in random mucosal biopsies from patients with bladder tumours. Scand J Urol Nephrol 14:37–41

Accepted August 18, 1984